Critical current density and magnetic behaviour of superconducting $YBa_2Cu_{3+y}O_{7-\delta}$: Ag_x composite

1991 J. Phys.: Condens. Matter 3 1181

(http://iopscience.iop.org/0953-8984/3/9/012)

J. Phys.: Condens. Matter 3 (1991) 1181–1187. Printed in the UK

Critical current density and magnetic behaviour of superconducting $YBa_2Cu_{3+y}O_{7-\delta}:Ag_x$ composite

D Sen†, S K Ghatak†, K L Chopra† and D Bhattacharya‡

† Department of Physics and Meteorology, Indian Institute of Technology, Kharagpur-721302, India

‡ Material Science Centre, Indian Institute of Technology, Kharagpur-721302, India

Received 11 June 1990, in final form 7 November 1990

Abstract. The effects of silver additive on the superconducting properties of $YBa_2Cu_{3+y}O_{7-\delta}:Ag_x$ for $x = 0.1$, 0.3, 0.6 and 1.2 are studied by measuring the real and imaginary components of the magnetic response in an AC field. The data are fitted to Bean's critical state model and are used to obtain the macroscopic critical current density. The magnetic susceptibility and critical current density are found to depend on the silver content whereas T_c remains essentially unchanged. For $x = 1.2$ the critical current density sharply increases below 77 K. The results suggest that the silver improves the properties of grain boundaries and enhances the intergranular coupling. The real part of the magnetic response is found to be a function of H_a/H^*, where H^* is the value of the field when the critical-state profile reaches the centre of the specimen.

1. Introduction

The high critical current density in the superconducting state of a material is an important requirement for many superconducting devices. Although a very high critical current density (about 10^6 A cm^{-2} at low temperatures) is found in the single-crystal state of the oxide superconductor Y–Ba–Cu–O, bulk materials generally have much lower values, far below the single-crystal limiting value. The low critical current density in single-phase polycrystalline samples is believed to originate mainly from the presence of weak links between grains. The intergranular coupling essentially determines the macroscopic current density flowing between the particles. The improvement in intergranular coupling can therefore enhance the macroscopic current density. The addition of silver (metallic or oxide) is widely used in this respect (Daslandes *et al* 1989, Pavuna *et al* 1988, Zhen-Peng Su *et al* 1989). The composite Y–Ba–Cu–O : Ag_x shows lower resistivity in the normal state without changing the transition temperature. The critical current density as measured directly (Zhen-Peng Su *et al* 1989) or estimated from magnetization data (Pavuna *et al* 1988) is found to increase with the addition of Ag. In this paper, we report results on the measurement of the AC response of Y–Ba–Cu–O : Ag_x for different

0953-8984/91/091181 + 07 $03.50

values of x and observe that the macroscopic shielding current density which is controlled by intergranular coupling is enhanced for large values of x.

2. Experimental details

2.1. Sample preparation

A powder specimen of $YBa_2Cu_{3+y}O_{7-\delta}:Ag_x$ was prepared by the coprecipitation method reported earlier (Pramanik *et al* 1988). A pellet of this sample was sintered under O_2 at 965 °C for about 20 h and is cooled to room temperature at a rate of 1 °C min^{-1}. A powder specimen of $YBa_2Cu_{3.1}O_{7-\delta}:Ag_{0.6}$ was also prepared by the explosive pyrophoric method (Bhattacharya *et al* 1990). This sample was sintered at 900 °C for 20 h and slowly (1 °C min^{-1}) cooled to room temperature. The samples were formed into cylindrical shapes for the magnetic measurements. Four samples with nominal composition $YBa_2Cu_{3.05}O_{7-\delta}:Ag_x$ with $x = 0.1, 0.3, 0.6, 1.2$ and a sintering temperature of 965 °C were studied. The other two samples with nominal composition $YBa_2Cu_{3.1}O_{7-\delta}:Ag_{0.6}$ prepared by the pyrophoric (sintered at 900 °C) and the coprecipitation (sintered at 975 °C) methods are also used to study the effect of the preparation procedure on the superconducting properties.

2.2. AC susceptibility measurements

The AC response of the sample was measured using the mutual inductance method at a low frequency (about 66 Hz). Samples of cylindrical dimensions with a length ranging from 1.2 to 1.5 cm and a small diameter (0.2–0.4 cm) were used for the measurement. A sinusoidal magnetic field of amplitude in the range $0\ \mathrm{Oe} < H_a \leqslant 30\ \mathrm{Oe}$ was applied along the length of the sample. A single receiver coil with 100 turns of 48 gauge copper wire was tightly wound around the central zone of the sample. The signal was detected with a two-phase lock-in amplifier (PAR-5209). The sample was placed within a cryorefrigerator assembly with a temperature-controlled facility. The temperature was measured using a calibrated Si-diode sensor with an accuracy of ±0.1 K.

3. Results and discussion

3.1. AC susceptibility and shielding current density

The onset transition temperature as measured from the appearance of the diamagnetic signal is around 92 K for all the silver-doped samples studied here. Typical results on the real and imaginary parts of the differential susceptibility χ for $x = 0.1$ (sample A) and $x = 0.6$ (prepared by the pyrophoric method; sample B) are shown in figures 1 and 2. In the presence of a small exciting field the transition is sharp and the real part χ_R of the susceptibility saturates at low temperatures. Its value at 60 K for the sample with $x = 0.6$ is -0.99 (sample B) and is higher than -0.89 for the sample with $x = 0.1$ (sample A). It is observed that the sample with $x = 0.6$ prepared following the pyrophoric route shows a much sharper transition and higher diamagnetic shielding than samples with the same amount of Ag obtained by the coprecipitation method and sintered at a different temperature. As the amplitude of excitation increases, the shielding decreases at low temperatures. The out-of-phase response (figures 1(*b*) and 2(*b*)) exhibits a peak below

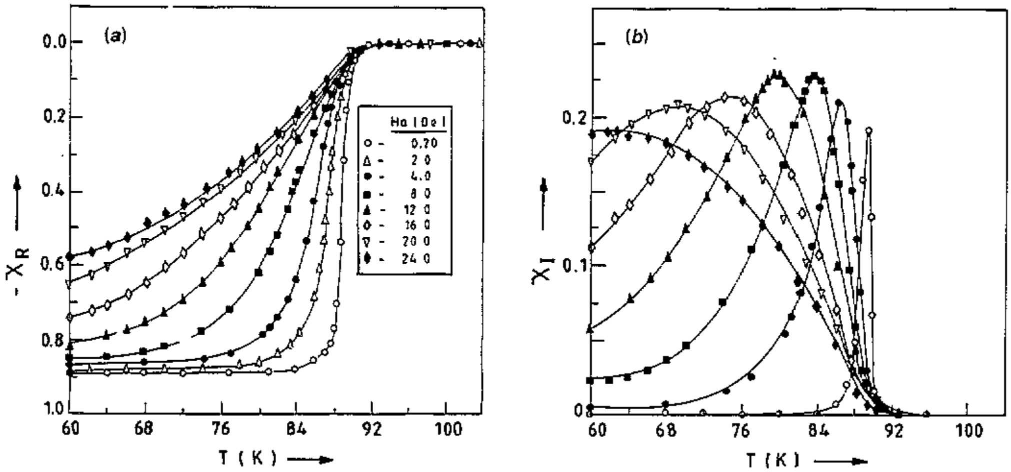

Figure 1. Temperature dependences of (*a*) the real part χ_R and (*b*) the imaginary part χ_I of the AC magnetic susceptibility for the bulk sample $YBa_2Cu_{3.05}O_{7-\delta}$:$Ag_{0.1}$ (sample A) at different excitation fields H_a. The values of H_a in (*a*) and (*b*) are the same and as given in the key.

T_c and its position shifts towards lower temperatures with higher excitation amplitudes. The sharpness of the peak is also a decreasing function of the excitation amplitude. The values of the measured quantities of these samples are given in table 1. As the peak in χ_I broadens with increase in the excitation field, the inaccuracy in estimating T^* where χ_I exhibits a maximum also increases. The maximum inaccuracy in T^* is ± 1.5 K. In Bean's (1964) model both χ_R and χ_I at $T = T^*$ are independent of the applied field. The experimental results on χ_I show that, within our experimental accuracy, χ_I is nearly constant although its values are found to be different for the two samples. The real part χ_R changes with H_a. In comparing observed values of χ_R, one must take into account the fact that, at around $T \simeq T^*$, χ_R is a steep function of temperature and hence the observed variation in χ_R with H_a at $T = T^*$ contains an estimation uncertainty. The general trend of the experimental result is in very good agreement with Bean's model. Similar variation in χ_R at T^* has been observed earlier for bulk Y–Ba–Cu–O (Murphy *et al* 1989, Hanic *et al* 1989).

The sintered material can be modelled as an array of granular materials where the grains are coupled to each other by weak links. For a temperature $T < T_c$, when the grains are phase locked, the macroscopic shielding current flows around the surface of the sample in the presence of a small magnetic field. For a field less than the intergranular lower critical field, the screening is nearly complete whereas, for a larger field, intergranular vortices are present in the sample. The magnetic response of this system can be derived using the critical-state model (Bean 1964, Clem 1988). The real part of the AC response measures the flux expelled at the peak value of the AC field whereas the imaginary part is determined by the trapped flux (Gomory 1989, Campbell 1969). For a cylindrical geometry the trapped flux has a maximum when the state has reached the centre of the sample and this occurs when the macroscopic critical current density $J_s(T^*) = H^*/R$ where H^* is the amplitude of the field and R the radius of the sample. The critical current density obtained from the maximum χ_I is plotted in figure 3. As the critical current density for $x = 0.3$ is comparable with that for $x = 0.1$, the results for $x =$

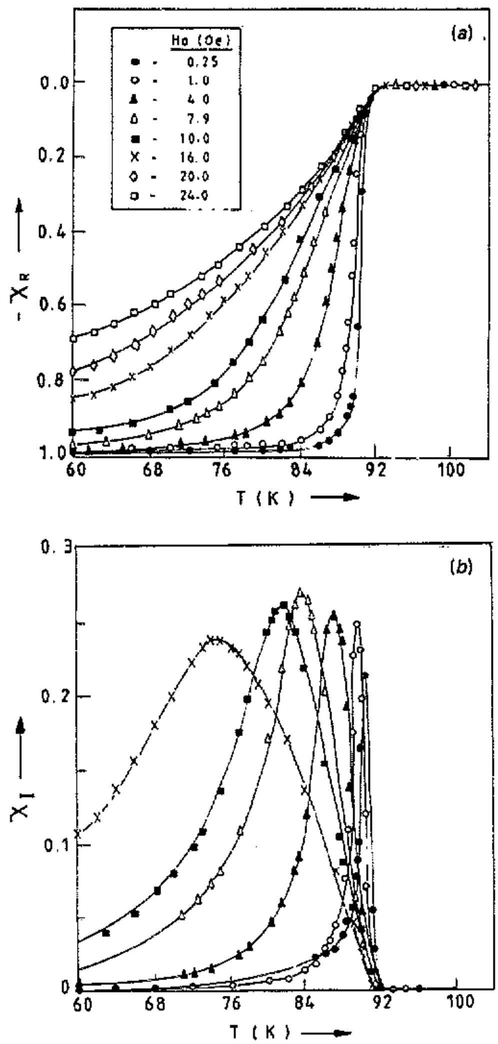

Figure 2. Temperature dependences of (*a*) the real part χ_R and (*b*) the imaginary part χ_I of the AC magnetic susceptibility for the sample $YBa_2Cu_{3.1}O_{7-\delta}:Ag_{0.6}$ (sample B) at different excitation fields H_a. The values of H_a in (*a*) and (*b*) are the same and as given in the key.

0.3 are not plotted. The samples having the same silver concentration ($x = 0.6$) but prepared by different routes show almost identical critical current densities near T_c, but at lower temperatures the shielding current density has a higher value for the sample sintered at a higher temperature. In particular a steeper increase in J_s is observed for the sample with $x = 0.6$ sintered at 975 °C. When the silver content is high ($x = 1.2$), the critical current density increases very sharply at low temperatures ($T < 77$ K). The microstructural analysis shows that the silver stays near the grain boundaries (Bhattacharya *et al* 1990). Therefore, the increase in the critical current density results from the improvement of the intergranular coupling due to the silver. The nature of the improvement of the current-carrying capacity of weak links depends on the types of

Table 1. Experimental data of AC susceptibility for the bulk samples.

H_a (Oe)	T^* (K)	$-\chi_R(T^*)$	$\chi_I(T^*)$	J_s ($A\,cm^{-2}$)
		$YBa_2Cu_{3.05}O_{7-\delta}:Ag_{0.1}$ (sample A)		
0.2	89.2	0.32	0.19	1
1.0	88.4	0.32	0.20	5
2.0	87.8	0.33	0.20	10
4.0	86.0	0.43	0.21	21
8.0	84.0	0.40	0.23	42
12.0	79.0	0.47	0.23	64
16.0	74.0	0.51	0.22	85
20.0	70.0	0.53	0.21	106
24.0	61.0	0.57	0.19	128
		$YBa_2Cu_{3.1}O_{7-\delta}:Ag_{0.6}$ (sample B)		
0.25	90.4	0.29	0.21	2
1.0	89.6	0.42	0.25	6
4.0	87.0	0.49	0.28	23
7.9	83.5	0.53	0.27	45
10.0	82.0	0.55	0.26	57
16.0	75.0	0.61	0.24	91
20.0	70.0	0.64	0.22	113
24.0	60.0	0.71	0.20	136

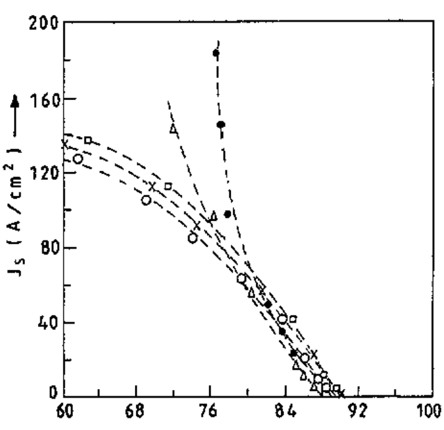

Figure 3. Temperature variation in the macroscopic shielding current density determined from AC susceptibility measurements on the samples: ○, $YBa_2Cu_{3.05}O_{7-\delta}:Ag_{0.1}$, sintering temperature $T_s = 965\,°C$; ×, $YBa_2Cu_{3.1}O_{7-\delta}:Ag_{0.6}$ (pyrophoric), $T_s = 900\,°C$; □, $YBa_2Cu_{3.05}O_{7-\delta}:Ag_{0.6}$, $T_s = 965\,°C$; △, $YBa_2Cu_{3.05}O_{7-\delta}:Ag_{0.6}$, $T_s = 975\,°C$; ●, $YBa_2Cu_{3.05}O_{7-\delta}:Ag_{1.2}$, $T_s = 965\,°C$.

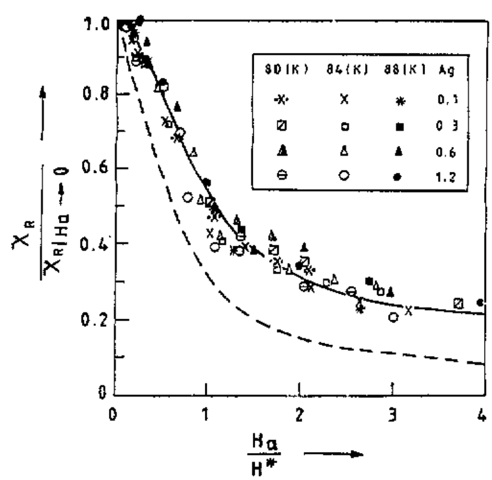

Figure 4. Variation in the real part $\chi_R(H_a)/\chi_R(H_a \rightarrow 0)$ of the response as a function of H_a/H^* for samples with different silver concentrations at temperatures of 80, 84 and 88 K: – – –, prediction of Bean's model with $\mu_{eff} = 1$; ———, a guide to the eye.

weak links. When the intergranular junctions are Josephson's weak links, the critical current I_c is given by (Ambegaokar and Baratoff 1963)

$$I_c = (\pi/eR_n)\Delta(T)\tanh[\Delta(T)/2kT]$$

where $\Delta(T)$ is the temperature-dependent energy gap parameter and R_n is the junction's normal-state tunnelling resistance. As the resistivity in normal state decreases with the addition of silver the junction resistance R_n is expected to be lowered because of the silver, resulting in a higher shielding current. The critical current vanishes following $I_c(T) \propto (1 - T/T_c)$ near T_c. When the suppression of the order parameter by the current is considered, the temperature variation in I_c changes to $I_c \propto (1 - T/T_c)^{3/2}$ (Clem *et al* 1987). If the links are superconductor–normal metal–superconductor (s–n–s) junctions, then the critical current $I_c = (1 - T/T_c)^2 \exp(-2d/\xi)$, where d is the thickness of the normal metal layer and ξ is the coherence length of electrons (Zhen-Peng *et al* 1989). Except for the first case the temperature variation shows that $(d^2I/dT^2)_{T_c} > 0$. This is also the case for a single s–n–i–n–s layer (where i stands for insulator). The results in figure 3 show that $(d^2I/dT^2)_{T_c} > 0$. Therefore, it is difficult to ascertain the exact nature of the weak links. From the microstructural evidence that most of the silver resides at the grain boundary in metallic form, the intergranular junction is expected to be of the type s–n–s. On the other hand, if the surface of the grain is oxygen deficient, the intergranular junction can be a combination of s–i–s and s–n–s junctions.

3.2. *Equation of state for the magnetic response*

In order to examine further the validity of Bean's model the field dependence of χ_R is examined in reduced units. In figure 4, $\chi_R(H_a)/\chi_R(H_a \to 0)$ is plotted against H_a/H^* for the temperatures $T = 80$, 84 and 88 K. We note that within the experimental accuracy the data show that $\chi_R(H_a)/\chi_R(H_a \to 0)$ is a unique function of H_a/H^*. We note that H^* is temperature dependent. In the same figure the result for cylindrical geometry as follows from Bean's model with $\mu_{eff} = 1$ (Clem 1988) is

$$\chi_R(H_a)/\chi_R(H_a \to 0) = \begin{cases} 1 - z(1 - \frac{5}{16}z) & \text{for } z \leqslant 1 \\ \frac{5}{16}/z & \text{for } z \geqslant 1 \end{cases}$$

where $z = H_a/H^*$ is also shown (broken curve). The experimental data lie above the theoretical curve with $\mu_{eff} = 1$ and thus correspond to the case with $\mu_{eff} < 1$.

4. Conclusion

The magnetic properties of bulk materials can be described within the critical-state model. The addition of silver enhances the intergranular coupling and the critical current density increases as the silver concentration increases. The magnetic response of the bulk superconducting state is found to be uniquely determined by H_a/H^* as follows from the critical-state model. The variation in $\chi_R(T^*)$ with applied field and the deviation of $\chi_R(H_a)/\chi_R(H_a \to 0)$ from Bean's result could be due to the field dependence of J_s. The effect of the field dependence of J_s on the unique behaviour of $\chi_R(H_a)/\chi_R(H_a \rightarrow 0)$ is being examined within Kim's model.

Acknowledgments

The technical help by Mr S Mazumder is gratefully acknowledged. The work is partly supported by the Department of Science and Technology, Government of India. D Sen is grateful to the Council of Scientific and Industrial Research for financial assistance.

References

Ambegaokar V and Baratoff A 1963 *Phys. Rev.* B **10** 486
Bean C P 1964 *Rev. Mod. Phys.* **36** 31
Bhattacharya D, Pathak L C, Mishra S K, Sen D and Chopra K L 1990 *Appl. Phys. Lett.* **57** 2145
Campbell A M 1969 *J. Phys. C: Solid State Phys.* **2** 1492
Clem J R 1988 *Physica* C **153–5** 50
Clem J R, Bumble B, Raider S J, Gallagher W J and Shih Y C 1987 *Phys. Rev.* B **35** 6637
Daslandes F, Raveau B, Dubots P and Leyat D 1989 *Solid State Commun.* **71** 407
Gomory F 1989 *Solid State Commun.* **70** 879
Hanic F, Polak M, Gomory F, Plesch G, Horvath I, Lobotka P and Galikova L 1989 *Br. Ceram. Trans. J.* **88** 35
Murphy S D, Renouard K, Crittenden R and Bhagat S M 1989 *Solid State Commun.* **69** 367
Pavuna D, Berger H, Affronte M, Vander Maas J, Capponi J J, Guillot M, Lejay P and Tholence J L 1988 *Solid State Commun.* **68** 535
Pramanik P, Biswas S, Singh C, Bhattacharya D, Dey T K, Sen D, Ghatak S K and Chopra K L 1988 *Mater. Res. Bull.* **23** 1693
Zhen-Peng Su, Yong Zhoo, Shi-Fang Sun and Zu-Yao Chen 1989 *Solid State Commun.* **69** 1067